$Ca_v1.4$ Encodes a Calcium Channel with Low Open Probability and Unitary Conductance

Clinton J. Doering,*† Jawed Hamid,* Brett Simms,* John E. McRory,* and Gerald W. Zamponi*

*Hotchkiss Brain Institute, Department of Physiology and Biophysics, Faculty of Medicine, University of Calgary, Calgary, Canada; and †NeuroMed Technologies, Vancouver, Canada

ABSTRACT When transiently expressed in tsA-201 cells, $Ca_v1.4$ calcium channels support only modest whole-cell currents with unusually slow voltage-dependent inactivation kinetics. To examine the basis for this unique behavior we used cell-attached patch single-channel recordings using 100 mM external barium as the charge carrier to determine the single-channel properties of $Ca_v1.4$ and to compare them to those of the $Ca_v1.2$. $Ca_v1.4$ channel openings occurred infrequently and were of brief duration. Moreover, openings occurred throughout the duration of the test depolarization, indicating that the slow inactivation kinetics observed at the whole-cell level are caused by sustained channel activity. $Ca_v1.4$ and $Ca_v1.2$ channels displayed similar latencies to first opening. Because of the rare occurrence of events, the probability of opening could not be precisely determined but was estimated to be <0.015 over a voltage range of -20 to $+20$ mV. The single-channel conductance of $Ca_v1.4$ channels was ~4 pS compared with ~20 pS for $Ca_v1.2$ under the same experimental conditions. Additionally, in the absence of divalent cations, $Ca_v1.4$ channels pass cesium ions with a single-channel conductance of ~21 pS. Although $Ca_v1.2$ opening events were best described kinetically with two open time constants, $Ca_v1.4$ open times were best described by a single time constant. BayK8644 slightly enhanced the single-channel conductance in addition to increasing the open time constant for $Ca_v1.4$ channels by ~45% without, however, causing the appearance of an additional slower gating mode. Overall, our data indicate that single $Ca_v1.4$ channels support only minute amounts of calcium entry, suggesting that large numbers of these channels are needed to allow for significant whole-cell current activity, and providing a mechanism to reduce noise in the visual system.

INTRODUCTION

The release of neurotransmitters at photoreceptor synapses is critically dependent on calcium entry via voltage-gated calcium channels. Unlike in many other types of synapses that show transient vesicular release in response to an action potential, vertebrate photoreceptors show evidence of tonic neurotransmitter release in the dark. In the absence of a light stimulus, photoreceptors exhibit a resting potential of ~−40 mV, resulting in constitutive L-type calcium channel activity and tonic glutamate release (i.e., see Schneeweis and Snapf (1) and Taylor and Morgans (2)). A light stimulus hyperpolarizes the photoreceptor, deactivates the L-type calcium channels, and consequently terminates glutamate release. To permit tonic glutamate release at resting membrane potentials, L-type channels need to be able to be continuously open, thus necessitating a large window current and resistance to voltage- and calcium-dependent inactivation.

It is now well established that $Ca_v1.4$ calcium channels are the predominant L-type calcium channel involved in glutamate release from rod photoreceptors (2–6). Mutations in the $Ca_v1.4$ gene have been associated with incomplete X-linked congenital stationary night blindness (CSNB2) (7–9), consistent with their key role in rod photoreceptor function. Functional expression of $Ca_v1.4$ calcium channels in tsA-201 cells (10–12) has revealed that $Ca_v1.4$ calcium channels support whole-cell currents with ultraslow inactivation kinetics in both calcium- and barium-containing recording solutions. This suggests that these channels may display prolonged single-channel activity during membrane depolarization. Interestingly, compared with other neuronal L-type calcium channel isoforms, whole-cell current amplitudes were found to be unusually small despite robust membrane expression as visualized by immunostaining (11). To determine the biophysical basis of the unique functional properties of $Ca_v1.4$, we carried out single-channel cell-attached patch recordings from transiently transfected tsA-201 cells. Our data show that $Ca_v1.4$ channels are reluctant to open, remain open only briefly, and display a single-channel conductance that is smaller than any known type of voltage-gated calcium channels. We suggest that significant calcium entry into rod photoreceptor terminals requires the expression of a large number of functional $Ca_v1.4$ channels, a characteristic of the unique ribbon synapse structure found in the retina (13,14).

MATERIALS AND METHODS

Cloning of human $Ca_v1.4$

Total RNA was isolated from the neuroblastoma cell line Y-79 using Trizol (Invitrogen, Carlsbad, CA) according to the manufacturer's instructions. Single-stranded cDNA was produced using oligo-$dT_{12–18}$ and superscript II (Invitrogen). This DNA preparation was amplified using oligos based upon the nucleotide sequence of published $Ca_v1.4$ cDNA in Genbank (National Center for Biotechnology Information; accession number AJ224874) and Klentaq LA (Clontech, Palo Alto, CA). The cDNA was produced in two

Submitted May 22, 2005, and accepted for publication July 19, 2005.

Address reprint requests to Dr. Gerald W. Zamponi or Dr. John McRory, Dept. of Physiology and Biophysics, University of Calgary, 3330 Hospital Dr. NW, Calgary, T2N 4N1 Canada. Tel.: 403-220-8687; Fax: 403-210-8106; E-mail: Zamponi@ucalgary.ca or Mcroryj@ucalgary.ca.

0006-3495/05/11/3042/07 $2.00

doi: 10.1529/biophysj.105.067124

fragments by polymerase chain reaction; a 5′ specific short fragment of ~500 nucleotides and another fragment of ~6 kb starting from the 3′ end of the 500-basepair fragment with some overlap. The two isolated fragments were then subjected to an A-tailing procedure using Taq DNA polymerase and 2 mM dATP. After A-tailing, the DNA fragments were isolated and cloned separately into the pGEM TEASY vector according to the manufacture's instructions. The plasmid DNA was isolated from the resulting clones, digested, and ligated to produce a full length $Ca_v1.4$ clone. The DNA was then excised and subcloned into the mammalian expression vector pcDNA3.1-zeo (Invitrogen). The resulting clone was sequenced fully from both directions, and is identical to the sequence reported by McRory et al. (11).

Culture and transient transfection of tsA-201 cells

The procedures for culturing, splitting and transfection of tsA-201 cells via the calcium phosphate method have been previously described by us in detail (11). In all experiments, human $Ca_v1.4$ or rat $Ca_v1.2$ calcium channel α_1 subunits were cotransfected with rat β_{2a}, rat α_2-δ_1 and enhanced green fluorescent protein (EGFP). In control cells, only the ancillary calcium channel subunits were expressed, whereas the α_1 subunit was omitted.

Electrophysiological measurements and data analysis

Single-channel recordings were performed using an Axopatch 200B amplifier (Axon Instruments, Foster City, CA) linked to a personal computer equipped with pClamp v9.0. Patch pipettes (Sutter borosilicate glass, BF 150-86-15, Sutter Instrument, Novato, CA) were pulled using a Sutter P-87 microelectrode puller, and fire-polished using a Narishige microforge (Tokyo, Japan) to a resistance of 10–20 MΩ. Pipettes were coated with sylgard and filled with solution containing either (in mM) 100 $BaCl_2$ and 10 HEPES (pH 7.2 with CsOH); 100 $CaCl_2$ and 10 HEPES (pH 7.2 with CsOH); or 100 $CsCH_3SO_3$, 10 HEPES, 10 EGTA, and 20 TEA-Cl (pH 7.2 with CsOH). Cells were bathed in a solution comprised of (in mM) 140 potassium gluconate, 1 $MgCl_2$, 10 HEPES, 10 EGTA, and 10 glucose (pH 7.3 adjusted with KOH) to set the membrane resting potential to 0 mV. Currents were elicited by stepping from a holding potential of −100mV (physiological) to various test depolarizations for 200 ms. The agonist BayK8644 (Sigma, St. Louis, MO) was dissolved in dimethylsulfoxide at a stock concentration of 10 mM, and perfused into the bath at a final concentration of 10 μM. Data were sampled at 5 kHz and filtered at 1 kHz during recordings, and then filtered an additional 500 Hz using a Gaussian filter during data analysis via Clampfit (Axon Instruments). Capacitative transients were compensated by subtraction of blank sweeps. For whole-cell recordings, cells were bathed in external solution consisting of (in mM) 100 $BaCl_2$, 15 CsCl, 1 $MgCl_2$, 10 HEPES, 10 glucose, 10 TEA-Cl, pH 7.2 with TEA-OH; electrodes (3–4 MΩ) were filled with internal solution consisting of (in mM) 108 $CsCH_3SO_3$, 4 $MgCl_2$, 9 EGTA, 9 HEPES, pH 7.2 with CsOH. I/V relationships were recorded by stepping from a holding potential of −100 mV to various test potentials for 200 ms. Whole-cell currents were filtered at 1 kHz and sampled at 2 kHz. All curve fittings were carried out in Sigmaplot 6.0 (Jandel Scientific, San Rafael, CA). Statistical analysis was carried out using SigmaStat 2.0 (Jandel Scientific) using Student's *t*-tests at the 0.05 level. Values reported are mean ± SE, and voltages indicated correspond to physiological potentials. * denotes significance at the 0.05 level, and ** at the 0.01 level (see Fig. 4 *A*).

RESULTS AND DISCUSSION

We recorded single-channel events for $Ca_v1.4$ and $Ca_v1.2$ channels under identical experimental conditions. Fig. 1 compares the single-channel activities of $Ca_v1.4$ and $Ca_v1.2$ calcium channels coexpressed with ancillary α_2-δ_1 and β_{2a} subunits in the absence of the agonist BayK8644 at three different voltages. Two major differences between the two channel types are evident. First, $Ca_v1.4$ calcium channels appear to open less frequently compared with $Ca_v1.2$ at all voltages examined. More strikingly, the amplitudes of the single-channel events observed with $Ca_v1.4$ channels appear considerably smaller than those seen with $Ca_v1.2$.

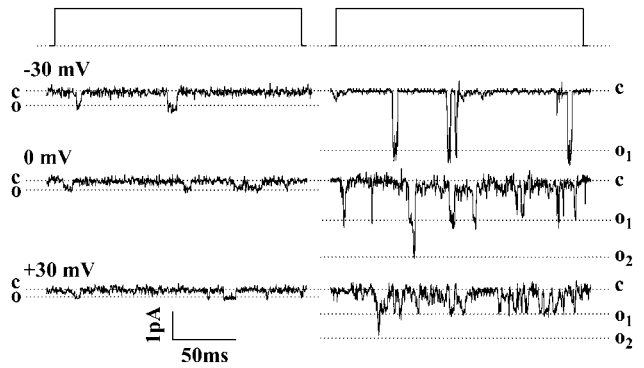

FIGURE 1 Single-channel openings observed for $Ca_v1.4$ (*left*) and $Ca_v1.2$ channels (*right*) when cotransfected with ancillary α_2-δ_1 and β_{2a} subunits. The events were recorded with 100 mM barium as the charge carrier in the absence of agonist BayK8644. The events were observed by depolarizing from a holding potential (physiological) of −100 mV to −30 mV (*top traces*), 0 mV (*middle traces*), and +30 mV (*bottom traces*). Dashed lines denote closed (*c*) and open (*o*) levels. Coincident openings are evident for $Ca_v1.2$ indicating that at least two channels were in the patch. Note that $Ca_v1.4$ channel openings are smaller in amplitude and occur less frequently than those observed with $Ca_v1.2$. Both records were filtered at the same frequency; the difference in noise is due to recordings having been performed at different times when the root mean-square noise differed.

This latter property is examined quantitatively in Fig. 2 in the form of averaged single-channel current-voltage relations for both channel types. As is clearly evident from the figure,

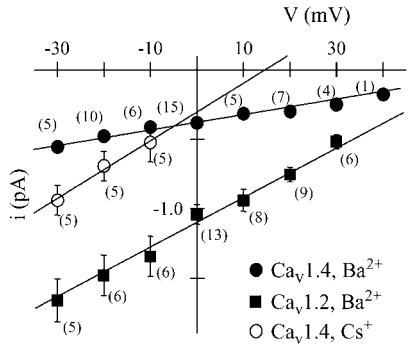

FIGURE 2 Current-voltage relations for single $Ca_v1.4$ (*circles*) and $Ca_v1.2$ (*squares*) channels, with either barium (*solid symbols*) or cesium (*open symbols*) as the charge carrier. Data points are average event amplitudes mean ± SE, and numbers in parentheses indicate number of cells (note that error bars for $Ca_v1.4$ data are too small to be visible). Linear regression indicates that the unitary conductance is 3.7 ± 0.3 pS for $Ca_v1.4$ and 19.5 ± 0.1 pS for $Ca_v1.2$ in barium, and 21 ± 2 pS for $Ca_v1.4$ in cesium. The observed values are statistically significantly different ($p < 0.05$).

the single-channel amplitude observed with $Ca_v1.4$ is significantly ($p < 0.05$) smaller than that observed with $Ca_v1.2$. When data were fitted using linear regression, the single-channel conductance obtained for $Ca_v1.2$ was 19.5 ± 0.1 pS, whereas that of $Ca_v1.4$ was ~5 times smaller (3.7 ± 0.3 pS) with Ba^{2+} as the charge carrier. For comparison, the reported single-channel conductance of T-type calcium channels under similar experimental conditions is on the order of 8 pS (for example, see 15–17), indicating that $Ca_v1.4$ channels have by far the smallest unitary conductance among all known types of voltage-gated calcium channels. This small conductance likely contributes to the fact that these channels support relatively small currents at the whole-cell level despite abundant protein expression at the cellular surface (11). To rule out the possibility that the single-channel activity observed with $Ca_v1.4$ could be mediated by an endogenously expressed calcium channel, cells were transfected with only the ancillary β_{2a} and α_2-δ_1 subunits and then subjected to cell-attached patch-clamp recordings. In one parallel transfection, whereas three out of four cells transfected with $Ca_v1.4$ displayed opening events, 14 out of 14 cells transfected with only the ancillary subunits showed no events. In a total of 83 such control cells depolarization to −20 mV never yielded any detectable single-channel activity when 100 mM barium was used as the charge carrier (see Table 1). Hence, we conclude that the single-channel activity observed with $Ca_v1.4$ is not due to an endogenously expressed calcium channel.

To further characterize the biophysical properties of $Ca_v1.4$ channels, we examined single-channel activity carried by charge carriers other than barium. When the monovalent cation cesium was used as the charge carrier, $Ca_v1.4$ channels displayed a unitary conductance of 21 ± 2 pS (Fig. 2), which is ~6-fold greater than that observed in barium. Again, no channel activity was observed with cesium in eight out of eight cells lacking the $Ca_v1.4$ subunit, whereas five out of five cells expressing $Ca_v1.4$ displayed activity. We also planned to record in external lithium; however, in lithium-containing solution extensive single-channel activity (presumably carried by potassium channels; see Zhu et al. and Avila et al. (18,19)) could be observed in control cells, and hence lithium current recordings were not pursued further. Finally, we attempted to record events in 100 mM calcium; however, in six cells examined we were unable to detect/resolve channel activity, likely because unitary conductance in calcium may be below the noise resolution of our experimental setup. Indeed, we know from our previous whole-cell recordings that switching from barium to calcium drastically reduces whole-cell current amplitude (11). We also note that our previous data showed that dropping the external calcium concentration to 2 mM further reduces whole cell currents, and hence, it is likely that the unitary conductance in physiological saline may be well below 1 pS.

TABLE 1 Summary of number of cells and sweeps (200-ms duration) for various transfection and recording conditions

Subunits transfected	Charge carrier	Cells with events (total No. of sweeps)	Cells without events (total No. of sweeps)
β_{2a}, α_2-δ_1	Ba^{2+}	None observed	83 (7916)
	Cs^+	None observed	8 (1200)
$Ca_v1.4$, β_{2a}, α_2-δ_1	Ba^{2+}	25 (5457)	13 (897)
	Ca^{2+}	None observed	6 (3397)
	Cs^+	5 (1250)	None observed
$Ca_v1.2$, β_{2a}, α_2-δ_1	Ba^{2+}	9 (2352)	None observed

Fig. 3 *A* depicts a series of continuous sweeps of channel activity obtained from a single patch expressing either a $Ca_v1.4$ or a $Ca_v1.2$ channel. Although $Ca_v1.2$ channel activity is evident during most sweeps, the patch containing $Ca_v1.4$ yielded predominantly blank sweeps. Fig. 3 *B* depicts an ensemble average obtained by pooling data from three different cells (from the same transfection) with a total of 600 sweeps out of which 39 contained single-channel events. As evident from the figure, the ensemble current waveform is qualitatively similar to that obtained from whole-cell recordings conducted in the same transfection and under the same ionic strength (i.e., 100 mM barium; see Fig. 3 *C*). It is important to note that despite pooling data from three cells, the total ensemble current amplitude is very small, consistent with the tiny single-channel conductance and low frequency of opening observed with $Ca_v1.4$. Note that the whole-cell currents required larger depolarizations to activate compared with the single-channel data, which may be due to dialysis of the cytoplasm during whole-cell recordings.

$Ca_v1.4$ activity could be observed at membrane potentials as negative as −30 mV (see Fig. 1), indicating that despite the high ionic strength used in our recordings, channel activity was evident at voltages close to the typical resting membrane potentials of a photoreceptor cell. However, events at this potential were infrequent, and hence kinetic analysis was restricted to potentials more positive than −30 mV. Fig. 4 *A* compares the fraction of sweeps that did not display opening events for $Ca_v1.4$ and $Ca_v1.2$ channels. At all potentials examined, $Ca_v1.4$ showed a significantly larger fraction of blank sweeps compared with $Ca_v1.2$ channels. Fig. 4 *B* examines the mean open times obtained from cumulative open time histograms. $Ca_v1.4$ activity was characterized by a single time constant at all potentials examined (−20 mV: $\tau_{open} = 2.97$ ms, $r^2_{fit} = 0.995$; 0 mV: $\tau_{open} = 3.03$ ms, $r^2_{fit} = 0.997$; +20 mV: $\tau_{open} = 3.35$ ms, $r^2_{fit} = 0.990$). In contrast, and in agreement with previous studies (20–23), two populations of opening events likely corresponding to two gating modes were evident for the $Ca_v1.2$ channel under identical experimental conditions, and hence cumulative open time histogram required a double exponential fit (−20 mV: $\tau_{open\ mode\ 1} = 3.71$ ms, $\tau_{open\ mode\ 2} = 63.8$ ms, $r^2_{fit} = 0.980$; 0 mV: $\tau_{open\ mode\ 1} = 4.30$ ms, $\tau_{open\ mode\ 2} = 22.1$ ms, $r^2_{fit} = 0.995$; +20 mV: $\tau_{open\ mode\ 1} = 3.63$ ms, $\tau_{open\ mode\ 2} = 153$ ms, $r^2_{fit} = 0.969$). Interestingly, the shorter time

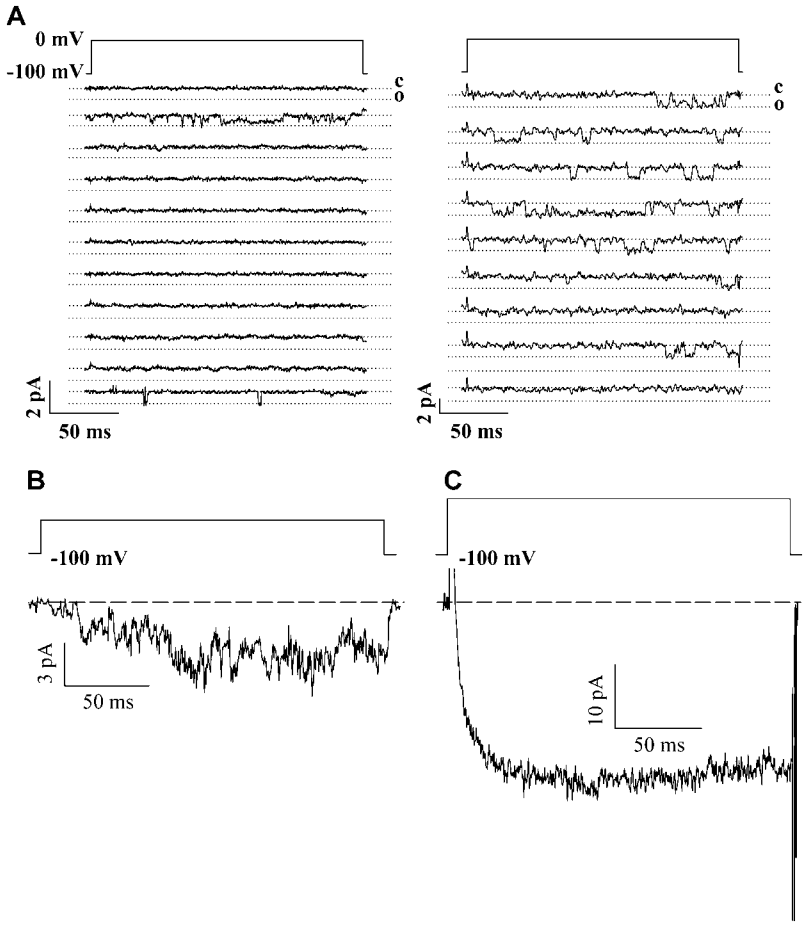

FIGURE 3 (*A*) Example of consecutive sweeps for $Ca_v1.4$ (*left*) and $Ca_v1.2$ (*right*). Note that events occur in relatively few traces with $Ca_v1.4$ and in most traces with $Ca_v1.2$. Traces were filtered at the same frequencies. (*B*) Ensemble current obtained by pooling data from three cells (600 sweeps, 39 of which showed events). Cells were from the same transfection. (*C*) Whole-cell current recorded in 100 mM external barium from the same transfection as the data shown in *B*. The test potential was +40 mV.

constant observed with $Ca_v1.2$ was similar to the open time constant determined for $Ca_v1.4$. Taken together, in addition to the lower fraction of blank sweeps observed with $Ca_v1.2$ (see Fig. 4 *A*), another major difference between the two channels is the apparent lack of a slow gating mode for $Ca_v1.4$. We note that data had to be filtered at 500 Hz during analysis to separate events from root mean-square noise due to the small single-channel conductance observed with $Ca_v1.4$. The corresponding filter dead time of 0.4 ms was therefore ~10-fold shorter than the mean open times. However, it is possible that brief closures may have been missed, and hence it is difficult to discriminate between single openings or very brief opening bursts, and to compare opening times obtained here with previous work on other types of L-type channels. For consistency within our own study, $Ca_v1.4$ and $Ca_v1.2$ data were filtered identically.

$Ca_v1.4$ is highly resistant to inactivation when currents are obtained in the whole cell configuration, with inactivation time constants of several seconds (10,11; Fig. 3 *C*). These observations can result from two distinct mechanisms: either $Ca_v1.4$ channels show continuous activity throughout the test depolarization or, alternatively, the latency to first opening could be longer than for other calcium channels and resulting late openings would appear as a slowing of inactivation at the whole-cell level. However, examination of first latency to opening time (t_{FL}; Fig. 4 *C*) indicates that both $Ca_v1.2$ and $Ca_v1.4$ channels display similar first latency distributions and, consequently, similar mean first latency times (τ_{FL}; Fig. 4 *D*). Therefore, the apparent lack of inactivation for $Ca_v1.4$ is most likely due to sustained channel activity (albeit at a low level) throughout the test pulse.

The infrequent occurrence of channel openings complicates quantitative analysis of the mean closed times of the $Ca_v1.4$ channel. Sweeps showing only one opening event cannot be utilized for analysis because the duration of the last closure within each sweep is skewed by the arbitrary termination of the sweep. Therefore, we analyzed closed times only for those sweeps that showed multiple channel openings, with the final closed event not being considered. In such sweeps, mean closed times of $Ca_v1.4$ were 33 ± 6 ms ($n = 52$) at −20 mV and 33 ± 10 ms ($n = 12$) at +20 mV, which are ~10-fold longer than the mean opening times.

Fig. 4 *E* examines the open probability of $Ca_v1.2$ and $Ca_v1.4$ channels at three different test potentials by calculating the ratio of total open time to total time. Here, we included all sweeps (including blank ones) up to the very last observable opening event for a given patch to ensure that any putative loss of channel activity would not skew our analysis.

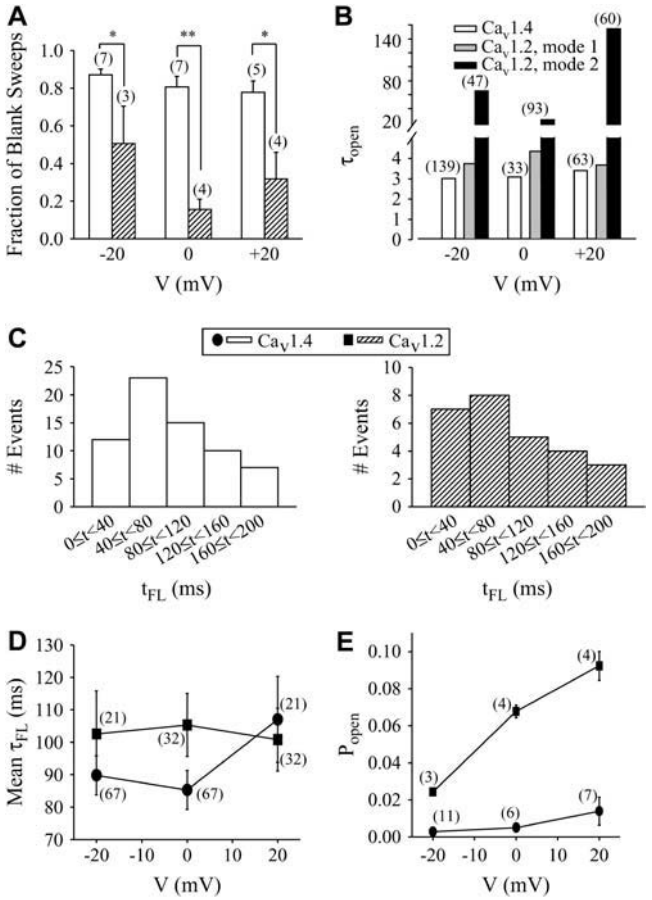

FIGURE 4 Analysis of single channel kinetics. (*A*) Fraction of blank sweeps for $Ca_v1.4$ and $Ca_v1.2$, at three different voltages. For a given cell, the number of sweeps containing no events was divided by the total number of sweeps (in this case, the total number was determined to be the sweep number in which the last event was observed), and this fraction averaged among different cells (indicated in parentheses). (*B*) Mean open times for $Ca_v1.4$ and $Ca_v1.2$ at three different test potentials determined from cumulative open time histograms. $Ca_v1.4$ events were best described by a single exponential fit, whereas $Ca_v1.2$ events required biexponential fits. Numbers in parentheses indicate total numbers of events in the open time histograms from which τ_{open} values were determined ($Ca_v1.4$, 15 cells; $Ca_v1.2$, 13 cells). (*C*) Histograms showing latency to first opening (t_{FL}) for $Ca_v1.4$ (*left*) and $Ca_v1.2$ (*right*) channels at −20 mV. Both $Ca_v1.4$ and $Ca_v1.2$ show similar first latency profiles. The bin width was 40 ms. (*D*) Mean first latency times for $Ca_v1.4$ and $Ca_v1.2$ channels. There was no statistical difference between the two channels. (*E*) Open probability of $Ca_v1.4$ channels determined from the ratio of total open time to total time for a given patch. Note that the open probability for $Ca_v1.4$ is more than 10-fold lower than for $Ca_v1.2$ channels (all values statistically significant, $p < 0.001$). Number in parentheses denotes number of cells.

P_{open} for $Ca_v1.4$ was determined to be 0.0029 ± 0.0007 ($n = 11$) at −20 mV, 0.005 ± 0.002 (n = 6) at 0 mV, and 0.014 ± 0.008 (n = 7) at +20 mV. In contrast, the open probability of $Ca_v1.2$ channels was ~10-fold higher (0.024 ± 0.002 ($n = 3$) at −20 mV, 0.068 ± 0.003 ($n = 4$) at 0 mV, and 0.092 ± 0.008 ($n = 4$) at +20 mV). Open probabilities of ~0.01 for $Ca_v1.4$ are qualitatively consistent with the observation that mean closed times were ~10 times greater than mean open times, and that 80–90% of all sweeps did not contain a channel opening. Moreover, the greater open probability for $Ca_v1.2$ is consistent with the smaller fraction of blank sweeps (Fig. 4 *A*) and longer opening events (Fig. 4 *B*).

We have shown previously that the application of BayK8644 results in an ~5-fold increase in $Ca_v1.4$ whole-cell currents (11). At the single-channel level, application of 10 μM BayK8644 to $Ca_v1.4$ channels resulted in a statistically significant increase in the single-channel amplitude (Fig. 5 *A*) with Ba^{2+} as the charge carrier, at a test potential of +20 mV, which is consistent with previous findings obtained with cardiac L-type channels (24). Additionally, τ_{open} as determined from the cumulative open time histogram (Fig. 5 *B*) increased by ~45% in the presence of the agonist, again with a monoexponential fit best describing the data. Similar results were obtained when Cs^+ was used as the charge carrier, with a 35% increase in τ_{open} at −20 mV ($n = 5$ cells, data not shown). These findings differ from previous results with other L-type calcium channel isoforms, where one of the major actions of BayK reportedly involves an enhancement of mode 2 gating (20). We did not observe similar mode 2 gating with $Ca_v1.4$ either in the absence or the presence of BayK, suggesting the possibility that this channel might lack this gating mode altogether.

The fraction of blank sweeps observed before BayK application (0.84 ± 0.01, $n = 4$) decreased significantly in the presence of BayK (0.65 ± 0.05, $n = 4$). This is different from what has been reported for other L-type calcium

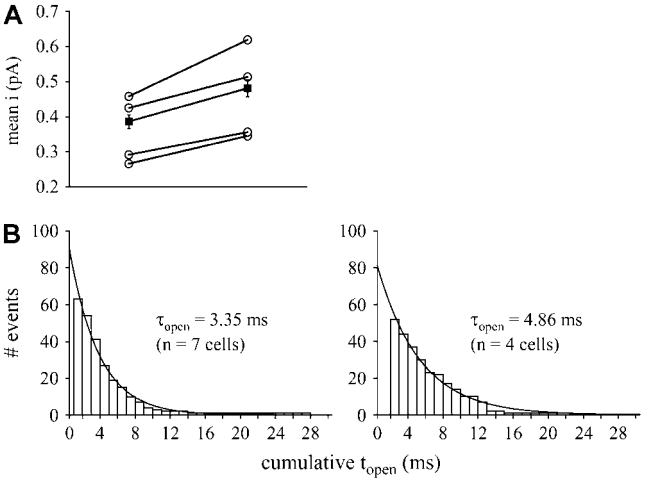

FIGURE 5 (*A*) Application of 10-μM BayK8644 increases single-channel amplitude at +20 mV. Hollow symbols indicate average data from individual cells, and the solid symbols indicate mean values with standard errors. Data in the presence and the absence of BayK were obtained from the same cells. BayK significantly increases the mean current from 0.39 ± 0.02 pA ($n = 26$ events) to 0.48 ± 0.02 pA ($n = 52$ events) ($p < 0.05$; paired Student's *t*-test). (*B*) BayK increases mean open time, τ_{open}. Cumulative open time histograms are shown in the absence (*left*) and presence (*right*) of BayK for events observed at +20 mV. The data are best described by a monoexponential fit ($r^2 = 0.99$ each). Here, the control data include cells that were not subsequently exposed to BayK.

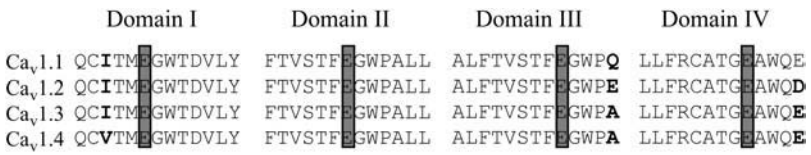

FIGURE 6 Alignment of p-loop regions of L-type calcium channels. Note that only one residue differs in each of domains I, III, and IV among the four family members, highlighted in bold. Glutamate residues thought to be important for selectivity are shown highlighted. Given the high sequence homology between $Ca_v1.2$ and $Ca_v1.4$, and the dramatically different unitary conductances and open probabilities, it is likely that residues outside of the pore region are important determinants in permeation.

channels, where alterations in the fraction of blank sweeps do not occur with BayK application, but are more typically observed through activation of intracellular messenger pathways (see, e.g., Tsien et al. (25) and Scamps et al. (26)). We do not know the molecular mechanisms by which BayK reduces the number of blank sweeps of $Ca_v1.4$, but these data further underscore the uniqueness of $Ca_v1.4$ among the family of L-type calcium channels.

The results shown in Figs. 1–5 are somewhat unexpected, given that amino acid residues comprising the putative selectivity filter region of $Ca_v1.4$ are highly conserved across all L-type voltage-gated calcium channels (Fig. 6). Although a charge substitution in the domain III region could account for the difference in conductance between $Ca_v1.2$ and $Ca_v1.4$, recordings of $Ca_v1.3$ (which shows this same loss of charge residue) from hair cells revealed similar conductances to those reported for $Ca_v1.2$ (see, e.g., Rodriguez-Contreras and Yamoah (27) and Kimitsuki et al. (28)). Therefore, there are likely additional determinants of ion permeation outside the very narrow region of the calcium channel pore that are responsible for the unique characteristics of $Ca_v1.4$. This is not without precedent, given that residues outside of the pore region in N-type calcium channels have been shown to affect permeation (29). Determination of the structural basis for these observed differences between $Ca_v1.4$ and $Ca_v1.2$ would require extensive mutagenesis analysis which, considering that each construct would have to be characterized at the single-channel level, is beyond the scope of this study.

Collectively, our data indicate that the single-channel properties of $Ca_v1.4$ channels are unique among L-type calcium channels. The ultra low open probability (i.e., <0.015) coupled with the unusually small unitary conductance implies that to obtain whole-cell currents in the 100-pA range, cells need to express large numbers of channels. This is consistent with the robust membrane expression of these channels as determined by immunofluorescence (11) but begs the question as to its possible physiological significance. Rod photoreceptor nerve terminals are unique in that they tonically release glutamate in the dark, which requires a continuous but precisely controlled influx of calcium ions via $Ca_v1.4$. These channels must be available for opening at rest (~ -35 to -40 mV) but display only a low level of activity to prevent calcium overload of the terminal. The ensemble of $Ca_v1.4$ channels operates within the window current range (11) and hence provides for a sustained and nonfluctuating inward calcium current. The small contribution of an individual $Ca_v1.4$ channel opening to the ensemble current ensures that calcium entry is protected from intrinsic fluctuations in channel activity, thus preserving a stable calcium influx into the photoreceptor terminal under low-light conditions—a critical feature of retinal signal transduction.

We thank Dr. Terry Snutch for providing rat calcium channel cDNAs.

This work was supported by operating grants to G.W.Z from the Canadian Institutes of Health Research and to J.E.M. from the Lions Sight Center. G.W.Z. holds a Canada Research Chair in Molecular Neuoscience and is a Senior Scholar of the Alberta Heritage Foundation for Medical Research. C.J.D. holds studentship awards from the Alberta Heritage Foundation for Medical Research and a Canada Graduate Scholarship from the Natural Sciences and Engineering Research Council.

REFERENCES

1. Schneeweis, D. M., and J. L. Schnapf. 1995. Photovoltage of rods and cones in the macaque retina. *Science*. 268:1053–1056.
2. Taylor, W. R., and C. Morgans. 1998. Localization and properties of voltage-gated calcium channels in cone photoreceptors of *Tupaia belangeri*. *Vis. Neurosci*. 15:541–552.
3. Corey, D. P., J. M. Dubinsky, and E. A. Schwartz. 1984. The calcium current in inner segments of rods from the salamander (*Ambystoma tigrinum*) retina. *J. Physiol.* 354:557–575.
4. Morgans, C. W. 2001. Localization of the α_{1F} calcium channel subunit in the rat retina. *Invest. Ophthalmol. Vis. Sci.* 42:2414–2418.
5. Haeseleer, F., Y. Imanishi, T. Maeda, D. E. Possin, A. Maeda, A. Lee, F. Rieke, and K. Palczewski. 2004. Essential role of Ca^{2+}-binding protein 4, a $Ca_v1.4$ channel regulator, in photoreceptor synaptic function. *Nat. Neurosci*. 7:1079–1087.
6. Barnes, S., and M. E. Kelly. 2002. Calcium channels at the photoreceptor synapse. *Adv. Exp. Med. Biol*. 514:465–476.
7. Strom, T. M., G. Nyakatura, E. Apfelstedt-Sylla, H. Hellebrand, B. Lorenz, B. H. Weber, K. Wutz, N. Gutwillinger, K. Ruther, B. Drescher, C. Sauer, E. Zrenner, T. Meitinger, A. Rosenthal, and A. Meindl. 1998. An L-type calcium-channel gene mutated in incomplete X-linked congenital stationary night blindness. *Nat. Genet.* 19:260–263.
8. Bech-Hansen, N. T., K. M. Boycott, K. J. Gratton, D. A. Ross, L. L. Field, and W. G. Pearce. 1998. Localization of a gene for incomplete X-linked congenital stationary night blindness to the interval between DXS6849 and DXS8023 in Xp11.23. *Hum. Genet.* 103:124–130.
9. Bech-Hansen, N. T., M. J. Naylor, T. A. Maybaum, W. G. Pearce, B. Koop, G. A. Fishman, M. Mets, M. A. Musarella, and K. M. Boycott. 1998. Loss-of-function mutations in a calcium-channel alpha1-subunit gene in Xp11.23 cause incomplete X-linked congenital stationary night blindness. *Nat. Genet.* 19:264–267.
10. Koschak, A., D. Reimer, D. Walter, J. C. Hoda, T. Heinzle, M. Grabner, and J. Striessnig. 2003. $Ca_v1.4$ α_1 subunits can form slowly inactivating dihydropyridine-sensitive L-type Ca^{2+} channels lacking Ca^{2+}-dependent inactivation. *J. Neurosci.* 23:6041–6049.
11. McRory, J. E., J. Hamid, C. J. Doering, E. Garcia, R. Parker, K. Hamming, L. Chen, M. Hildebrand, A. M. Beedle, L. Feldcamp, G. W.

Zamponi, and T. P. Snutch. 2004. The CACNA1F gene encodes an L-type calcium channel with unique biophysical properties and tissue distribution. *J. Neurosci.* 24:1707–1718.

12. Baumann, L., A. Gerstner, X. Zong, M. Biel, and C. Wahl-Schott. 2004. Functional characterization of the L-type Ca^{2+} channel $Ca_v1.4$ α_1 from mouse retina. *Invest. Ophthalmol. Vis. Sci.* 45:708–713.
13. Morgans, C. W. 2000. Presynaptic proteins of ribbon synapses in the retina. *Microsc. Res. Tech.* 50:141–150.
14. Zenisek, D., V. Davila, L. Wan, and W. Almers. 2003. Imaging calcium entry sites and ribbon structures in two presynaptic cells. *J. Neurosci.* 23:2538–2548.
15. Fox, A. P., M. C. Nowycky, and R. W. Tsien. 1987. Single-channel recordings of three types of calcium channels in chick sensory neurones. *J. Physiol.* 394:173–200.
16. Perez-Reyes, E., L. L. Cribbs, A. Daud, A. E. Lacerda, J. Barclay, M. P. Williamson, M. Fox, M. Rees, and J. H. Lee. 1998. Molecular characterization of a neuronal low-voltage-activated T-type calcium channel. *Nature.* 391:896–900.
17. Umemiya, M., and A. J. Berger. 1995. Single-channel properties of four calcium channel types in rat motoneurons. *J. Neurosci.* 15:2218–2224.
18. Zhu, G., Y. Zhang, H. Xu, and C. Jiang. 1998. Identification of endogenous outward currents in the human embryonic kidney (HEK 293) cell line. *J. Neurosci. Methods.* 81:73–83.
19. Avila, G., A. Sandoval, and R. Felix. 2004. Intramembrane charge movement associated with endogenous K^+ channel activity in HEK-293 cells. *Cell. Mol. Neurobiol.* 24:317–330.
20. Hess, P., J. B. Lansman, and R. W. Tsien. 1984. Different modes of Ca channel gating behaviour favoured by dihydropyridine Ca agonists and antagonists. *Nature.* 311:538–544.
21. Feldmeyer, D., W. Melzer, B. Pohl, and P. Zollner. 1990. Fast gating kinetics of the slow Ca^{2+} current in cut skeletal muscle fibres of the frog. *J. Physiol.* 425:347–367.
22. Pietrobon, D., and P. Hess. 1990. Novel mechanism of voltage-dependent gating in L-type calcium channels. *Nature.* 346:651–655.
23. Ma, J., A. Gonzalez, and R. Chen. 1996. Fast activation of dihydropyridine-sensitive calcium channels of skeletal muscle. Multiple pathways of channel gating. *J. Gen. Physiol.* 108:221–232.
24. Lacerda, A. E., and A. M. Brown. 1989. Nonmodal gating of cardiac calcium channels as revealed by dihydropyridines. *J. Gen. Physiol.* 93:1243–1273.
25. Tsien, R. W., B. P. Bean, P. Hess, J. B. Lansman, B. Nilius, and M. C. Nowycky. 1986. Mechanisms of calcium channel modulation by β-adrenergic agents and dihydropyridine calcium agonists. *J. Mol. Cell. Cardiol.* 18:691–710.
26. Scamps, F., B. Nilius, J. Alvarez, and G. Vassort. 1993. Modulation of L-type Ca channel activity by P2-purinergic agonist in cardiac cells. *Pflugers Arch.* 422:465–471.
27. Rodriguez-Contreras, A., and E. N. Yamoah. 2001. Direct measurement of single-channel Ca^{2+} currents in bullfrog hair cells reveals two distinct channel subtypes. *J. Physiol.* 534:669–689.
28. Kimitsuki, T., T. Nakagawa, K. Hisashi, S. Komune, and S. Komiyama. 1994. Single channel recordings of calcium currents in chick cochlear hair cells. *Acta Otolaryngol.* 114:144–148.
29. Feng, Z. P., J. Hamid, C. Doering, S. E. Jarvis, G. M. Bosey, E. Bourinet, T. P. Snutch, and G. W. Zamponi. 2001. Amino acid residues outside of the pore region contribute to N-type calcium channel permeation. *J. Biol. Chem.* 276:5726–5730.